Experimental and CFD Analysis of Heat Transfer Performance in Pulsating Heat Pipes by using Intermediate Temperature Fluids.

Sachin Govind Savant[1], Sunil Jagannath Kadam[2], Avinash H Kolekar[3], Chandrashekara M S[4], R Karthick[5], Rajesh Holkar[6], Vaibhav Harishchandra Bansode[7], Rudresha S[8]

[1]Department of Engineering Science, International Institute of Information Technology , Hinjawadi Pune - 411057 India.

[2]Department of Mechanical Engineering, Bharati Vidyapeeth College of Engineering, Kolhapur. 416013 India.

[3]Department of Mechanical Engineering, Vidya Pratishthan Kamalnayan Bajaj Institute of Engineering and Technology, Baramati,India

[4]Department of Computer Science and Engineering (Data Science), Maharaja Institute of Technology Mysore, Belawadi, Naguvanahalli, Srirangapatna Taluk, Mandya District, Karnataka - 571438, India.

[5]Department of Mechanical Engineering, Rajalakshmi Institute of Technology, Kuthampakkam , Poonamalle, Chennai - 600124,India.

[6]Department of Mechanical Engineering, Visvesvaraya Technological University, Belagavi, Karnataka, India

[7]Department of Mechanical Engineering, Sinhgad Academy of Engineering, Pune-48, India.

[8]Department of Mechanical Engineering, University of Visvesvaraya College of Engineering, Bengaluru, Karnataka, India

ABSTRACT

The study of turbulent pulsating flow and heat transfer is important for the study of the thermal hydraulic behavior of nuclear reactors in the maritime environment. The flow and heat transmission of turbulent pulsating flow are studied in this paper. The flow and heat transmission of the turbulent pulsating flow are not affected by the rolling axis and radius. The effect of the velocity oscillation period on the heat transmission is not as important as the effects of the Reynolds number and the oscillating velocity Reynolds number. The dependability of the CFD model is demonstrated by comparing the expected heat production and temperature distribution with the experimental results at the steady-state condition. The CFD model can be utilized to simulate the liquid up throwing phenomenon and the effect of the formation of hydrogen buffers on the heat transmission process. The formation of a gas blanket on the inner surface of the condenser is a result of the migration of hydrogen and the return of the condensate, which affects the heat transmission process negatively.

Keywords: Closed Loop Pulsating Heat Pipe, CFD Analysis, Liquid-Vapor Pulsating Flow.

1. Introduction

Though conventional heat pipes are available in a range of designs, market trends are often a reflection of their limitations. This has led to the creation of new concepts that are tailored to the requirements of the contemporary market. Pulsating or loop-type Heat pipes (PHP), a newly developed technology, falls into this category, according to Akachi [3, 4]. As a result of their superior operational characteristics and relatively lower costs, it is envisaged that this range of devices is likely to meet the contemporary, as well as the likely future, specific requirements of the electronics cooling industry.

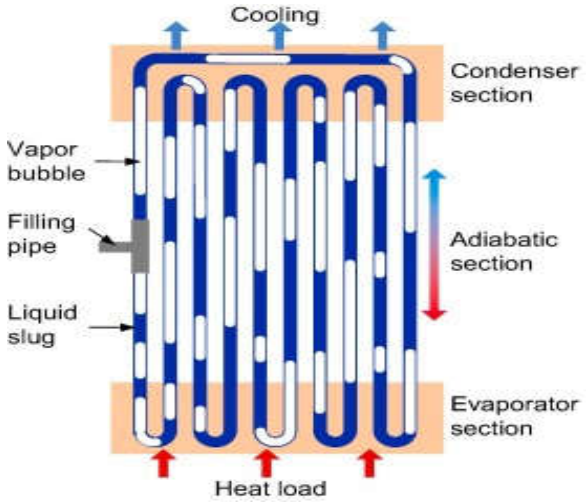

Figure 1. Block Diagram of Pulsating Heat Pipe.

Evaporation section, condensation section, and adiabatic section are major parts of the PHP structure. In fact, the condensation section usually touches the cooling system, and the evaporation section usually touches the heat source. The adiabatic section is used to calculate the lengths of these sections in the performance of the PHP. For example, an experiment was conducted by Kim et al. [24] to investigate the performance of the PHP when the condensation section's length was changed. The results showed that when the temperature in the condensation section was low, the temperature in the evaporation section decreased as well as the condensation section. If the temperature in the condensation section was high, the length of the condensation section was reduced by half, increasing the temperature in the evaporation section. However, Wang et al. [37] used a 2D CFD model to investigate the effect of the lengths of the evaporator and condenser on the performance of the single-loop PHP and found that shortening the condenser length was favorable for the start-up process in the heat pipe.

On conducting a variety of research, Khedekar et al. [5-7] came to a conclusion that working fluids, evaporation/condensation length, inner diameters, and turns are primary factors affecting heat transmission capabilities. They also demonstrated the effect of input heat flux and came to a conclusion that thermal resistance reduces smoothly with an increase in heat input.CFD

analysis is carried out by using volume of fluid models to analyze the effect of continuous-continuous phase interaction by considering a transient two-phase model to analyze the effect of change in length of evaporator section on thermal resistance and startup performance.

2. Intermediate Temperature Fluids Life Tests.

Intermediate temperature fluids are working fluids that are used in the temperature range between low-temperature fluids such as water and high-temperature liquid metals such as sodium. The temperature range for these fluids is between 400K and 750K. These fluids are necessary for use in situations in which water is ineffective due to high vapor pressures and low surface tension, yet the temperature is too low for the use of alkali metals due to low vapor velocities.

2.1. Common Types of Intermediate Temperature Fluids.

The search for such fluids is a challenging task in this range of temperatures due to problems such as thermal decomposition, high viscosity, and corrosiveness of fluidsOrganic Fluids: These fluids are often utilized in the lower end of this intermediate range, up to.Examples: Naphthalene, Toluene, Diphenyl, and Diphenyl Oxide, such as Dowtherm A/Therminol VP-1.
Limitations: They begin to decompose and liberate non-condensable gases (NCG) during higher temperatures. Halides: Compounds of elements with halogen families (fluorine, chlorine, bromine, iodine).Examples: Antimony Tribromide, Titanium Tetrachloride, and Aluminum Tribromide.Benefits: They are less likely to degrade and have high "Merit numbers" (efficiency indicators) in this temperature range. Elemental Fluids: Some of them have been tested and considered for specialized application. Examples: Mercury (toxic but stable), and mixtures of Sulfur and Iodine. Limitations: Sulfur is known to have extremely high viscosity, and mercury is known to have high toxicity and "wetting" issues. The intermediate temperature region is defined over a temperature range of 450 to 750 K. At temperatures above 700-725 K, alkali metal heat pipes begin to become effective. As temperature is reduced, vapor density and vapor pressure of alkali metals are reduced. At temperatures lower than 725 K, vapor density is reduced to such an extent that it is limited by sonic velocity of vapor.

Heat transfer:

The heat pipe (or LHP) vapor velocity is too high to be useful for the alkali metals in the intermediate temperature range. Historically, water has been used in heat pipes for temperatures up to about 425 K. Recently, it has been demonstrated that water can be used in heat pipes for temperatures up to 550 K using titanium or Monel envelopes (Anderson et al., 2006). Though water heat pipes can be used for temperatures as high as 550 K, the heat pipe effectiveness starts

to fall off above 500 K due to the decrease in the water's surface tension. As the heat pipes for the alkali metals are needed for temperatures above 700 K, and water heat pipes are needed for temperatures below 500 K, we have focused in this research on working fluids in the temperature range of 500 to 700 K. Several workers have suggested that halides could be used as working fluids in the intermediate temperature range (Saaski and Owarski, 1977; Saaski and Hartl, 1980; Anderson et al., 2004; Devarakonda and Olminsky, 2004; Devarakonda, Anderson, and Beach, 2005; and Locci et al., 2005). Life tests need to be accomplished before these working fluids can be reliably used.

There are a number of applications that could utilize heat pipes or loop heat pipes (LHPs) at intermediate temperatures ranging from 450 to 750 K, including space nuclear power system radiators, fuel cells, geothermal power, waste heat recovery systems, and high-temperature electronics cooling. The working fluids that could be used include organic fluids, elements, and halides. The paper also reviews previous life tests that have utilized 30 different intermediate-temperature working fluids, and over 60 different working fluid/envelope combinations. Life tests have also been performed with three different elemental working fluids, namely sulfur, sulfur-iodine mixtures, and mercury. However, other fluids have significant advantages over these three fluids at intermediate temperatures. Life tests have also been performed with 19 different organic fluids. As the temperature increases, all of them start to decompose. In most cases, they produce non-condensable gases, and in most cases, the viscosity also increases. The upper limit of the temperature depends on the amount of non-condensable gases that can be tolerated, as well as the life of the heat pipes. The highest long-term life tests were performed at 623 K (350°C), and short-term tests were performed at up to 653 K (380°C). Three groups of organic fluids appear to be promising as intermediate temperature fluids: (1) Diphenyl, Diphenyl Oxide, and Eutectic Diphenyl/Diphenyl Oxide, (2) Naphthalene, and (3) Toluene. While a fluorinating organic compound improves their stability, this effect has not been verified in life tests. Property data are lacking on the halides. The life tests currently in progress suggest that the halides may be suitable fluids at temperatures up to 673 K (400°C).Three groups of organic compounds are considered to be promising as intermediate temperature fluids. These are: (1) Diphenyl, Diphenyl Oxide, and Eutectic Diphenyl/Diphenyl Oxide, (2) Naphthalene, and (3) Toluene. Although it is postulated that the fluorination of organic compounds increases their stability, this effect needs to be verified during life tests. The life tests currently in progress indicate that the halides could be considered for use up to 673 K (400°C). However, there are gaps in the available data on the properties of the halides.

3: Physical and Governing Eq.

3.1: Physical model

Volume fluid model has been chosen to analyze the continuous-continuous interaction of two-phase flow and to predict the thermal performance. PHP is kept in a vertical position to get proper assistance from gravity. Evaporator section is kept at the bottom, the adiabatic section in the middle, and the condenser section at the top. The total length of the PHP has been kept constant, i.e., 100mm. The length of the adiabatic section has been kept constant. When the length of the evaporator section varies, the length of the condenser section varies accordingly, as the total length of the PHP has to be kept constant. Water has been chosen as the working fluid in the model. The liquid phase is taken as the primary phase, the vapor phase as the secondary phase, and the value of FR is 60%. The equation for the relationship between water's saturation temperature and pressure is given by: Tsat = 21.51ln(Pv) 2.7489, where Pv is the water's saturation temperature in degrees Celsius and Kpa is the absolute pressure. Adhesion between the liquid and the pipe's wall is taken into account when finding the value of the contact angle; this value is set at 20°.For a liquid and vapour plug to be created, the diameter has to be small enough for the liquid slug to dominate the gravitational action. When the square of the Bond number equals 4, the maximum diameter for a capillary tube is achieved.T h e B o n d n u m b e r The formula for the bond number can be rewritten to obtain the maximum inner diameter for the PHP, and we obtain

$$D_{crit} = 2\sqrt{\frac{\sigma}{g(\rho_l - \rho_v)}} \quad \text{.....2}$$

Sudden contraction or turn can also increase the losses and thereby affect the flow pattern. Sharp edges can also affect the flow pattern by creating separating capillary, which reduces the heat transfer capacity of the PHP. The critical diameter was calculated for various fluids, and it was between 3 to 5 mm. The diameter of the tube must be less than the critical diameter for the formation of slug. Hence, the diameter is taken as 2 mm.

3.2.Governing equations.

The two-phase for pulsating heat pipe has been simulated by VOF. VOF stands for the volume of fluid method, which is a free surface modelling technique. This model can be applied to two

or more kinds of non-mixed fluid. The fluid is divided into different analysis domains by the VOF model. In this case, the total volume fractions for the vapour phase and liquid phase in each domain add up to 1. In Eq. 1, the vapour phase and liquid phase are represented by the subscripts v and l.

For equation

$$\alpha_v + \alpha_l = 1 \ldots\ldots 3$$

The continuity equation, the momentum equation, and the energy equation are the governing equations for the two-phase flow of vapor and liquid mixtures. The continuity equation for the vapor-liquid two-phase mixture is given by the following equations:

For equation

$$\frac{\partial \alpha_l}{\partial t} + \nabla(\alpha_l \bar{v}) = \frac{S_{m,l}}{\rho_l} \ldots\ldots\ldots 4$$

$$\frac{\partial \alpha_v}{\partial t} + \nabla(\alpha_v \bar{v}) = \frac{S_{m,l}}{\rho_v} \ldots\ldots\ldots 5$$

3.4.Oscillating Motion of One Vapor Bubble and One Liquid Plug.

A typical OHP requires a relatively tiny tube diameter for the surface tension to produce liquid plugs and vapor bubbles. The oscillatory motion generated by the system is driven by the vapor bubbles present in the OHP. It is assumed that all the liquid plugs and the vapor bubbles act as a single entity. The heat transfer will take place through the walls and reach the working fluid when it is added to the evaporator section. The saturated liquid will change to saturated vapor during the process. The pressure of the vapor present in the evaporator section, pe, can be found by applying the Clapeyron equation if the temperature of the vapor present in the evaporator section, T_e, is known.

$$P_e = P_0 e^{\left[\frac{h_{lv} T_e - T_0}{R T_e T_0}\right]} \ldots\ldots 5$$

Utilizing a Taylor series and neglecting high-order terms, Eq 5 can be simplified as

$$\nabla P = P_e - P_c = P_c \left[e^{\frac{h_{lv} T_e - T_0}{R T_e T_0}} - 1 \right] \ldots\ldots\ldots 6$$

where T, which is equivalent to T 1/4 Te Tc, represents the temperature difference between the condensing and evaporating sections. Since the vapour trapped between liquid slugs is compressible, the resulting volume expansions and contractions in the vapour space cause an

oscillating effect, which influences the saturation temperatures in the evaporating and condensing sections. When the maximum temperature difference between two sections is Tmax, whereas the minimum temperature difference between two sections is Tmin, the temperature difference between the condensing part and the evaporating part will fluctuate within a range from Tmax to Tmin. When the frequency of system oscillation is, it is expected that the variation in temperature difference between the evaporating part and condensing part will be smaller when reference temperature and pressure are given by T0 and p0, respectively. Similarly, the temperature of the vapour in the condensing part, Tc, can be used to obtain an estimate of the vapour pressure, pc, in the condenser part by a similar approach. Consequently, the pressure difference between the condensing part and the evaporating part can be determined by which uses a Taylor series and ignores high-order terms, can be reduced to

$$\nabla P = \Delta T^{\lambda_{lv} \rho_{vc} T_r} \quad \text{.....7}$$

4.Geometric model.

The design of CFD Model of PHP is done in Ansys geometry, as shown in Fig 2. The design of CLPHP (Closed Loop Pulsating Heat Pipe) is done. It consists of a single loop of capillary material with dimensions (Inner Día: 2.0 mm, Outer Día: 5 mm). Copper is selected as material for better heat transfer. Length of adiabatic section is 40 mm. Length of evaporator and condenser section is 20 mm, 40 mm initially. Distance between tubes is 20 mm.

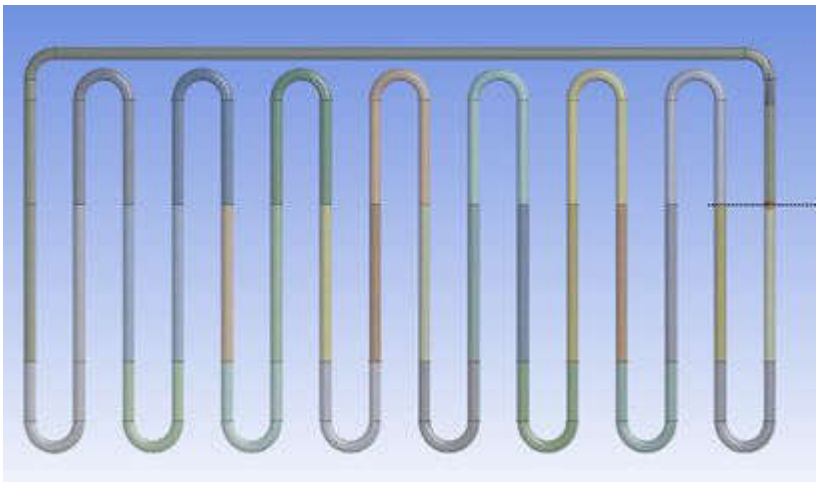

Fig: 2. Geometric model of Evaporator

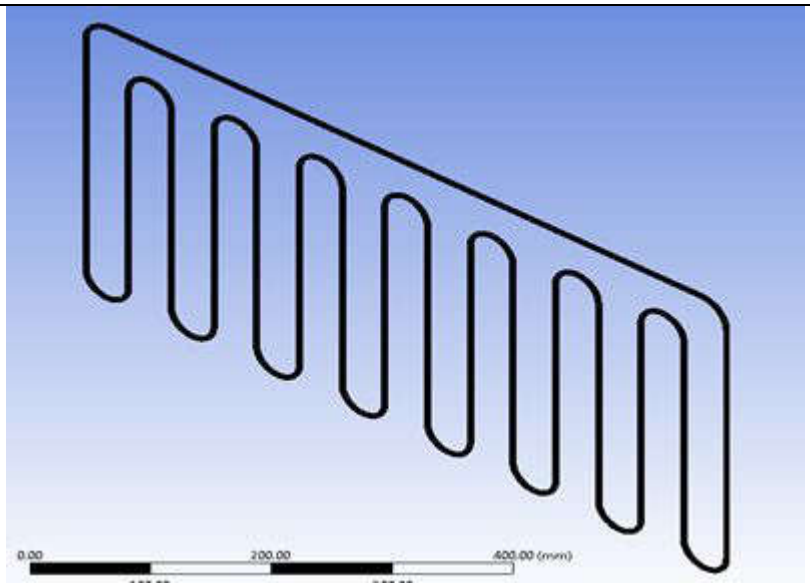

Fig .3. Meshing of Pulsating Heat Pipe.

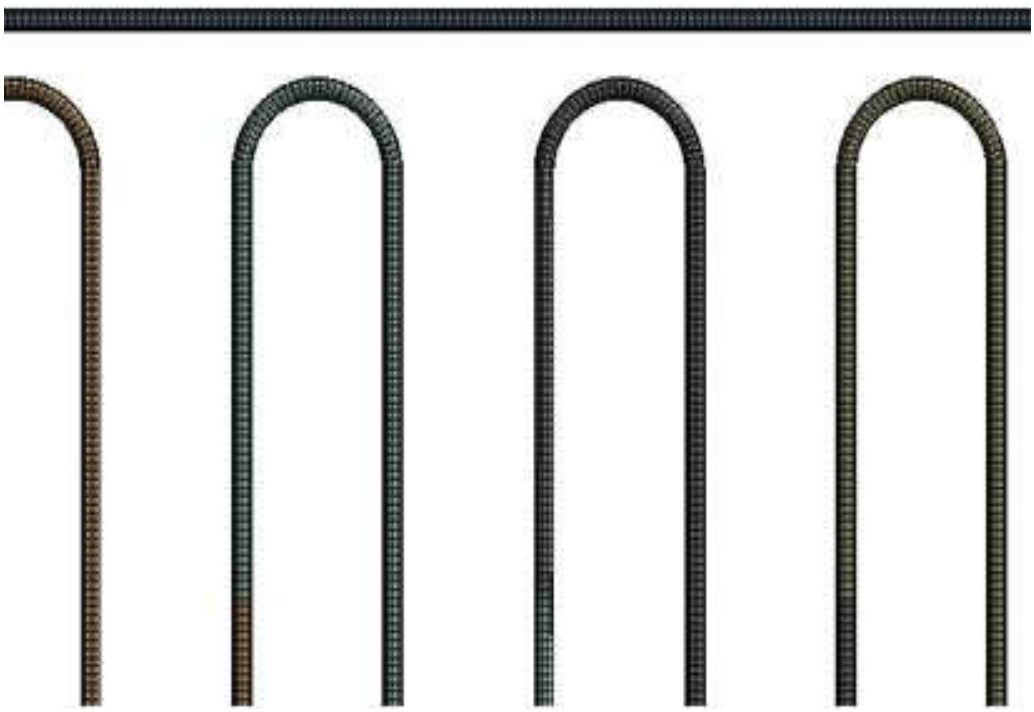

Fig: 4: Meshing of Closed Loop Pulsating Heat Pipe.

4.1.Meshing.

ANSYS A numerical grid is applied to a fluid body and its boundary during meshing, and this provides further control to a user in defining various combinations of point, edge, surface, and body controls. Applying a fine mesh with a cell count of 202836 and an element length ranging from 0.025 mm to 0.05 mm is generated. A mesh model of the evaporator section is shown in Figure 4.

.

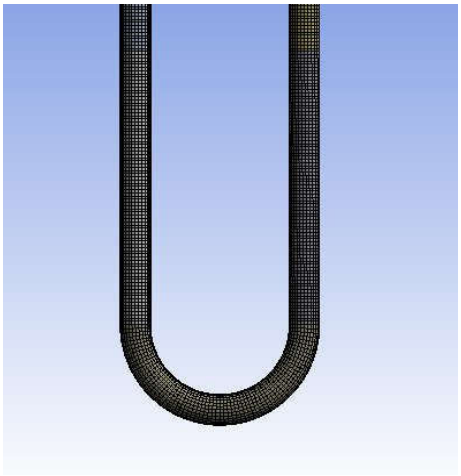

Fig.5 Mesh generation in evaporator section.

4.2. Boundary condition.

An alternative time condition has been selected. The model for the viscous fluid is the turbulent k-epsilon with the improved wall function. The temperature of the wall surfaces of the pipe is set to 303 K to create the first vapour-liquid dispersion. The fluid inside the pipe will eventually acquire the original distribution of the liquid columns and vapour plugs. Then, constant heat flux is specified to the evaporation section. The power input will affect the heat input to the condensation section, which will be at constant temperature (303).As per the normal temperature requirement for electronic cooling and the experimental results obtained by Lin et al. [16], the heating power for simulation is less than 90 watts. The vapour formation begins when the working fluid attains its boiling point, which has been set at 60 degrees Celsius with a filling ratio of 60%. A number of assumptions were made in the development of the model. These are:

(1) Surface tension is constant for the phases.

(2) The vapor phase is a perfect compressible gas, and the liquid phase is an incompressible fluid.

(3) The liquid phase has a constant density and a constant specific heat capacity.

(4) The heat input into the evaporator is constant.

5. Experimental setup.

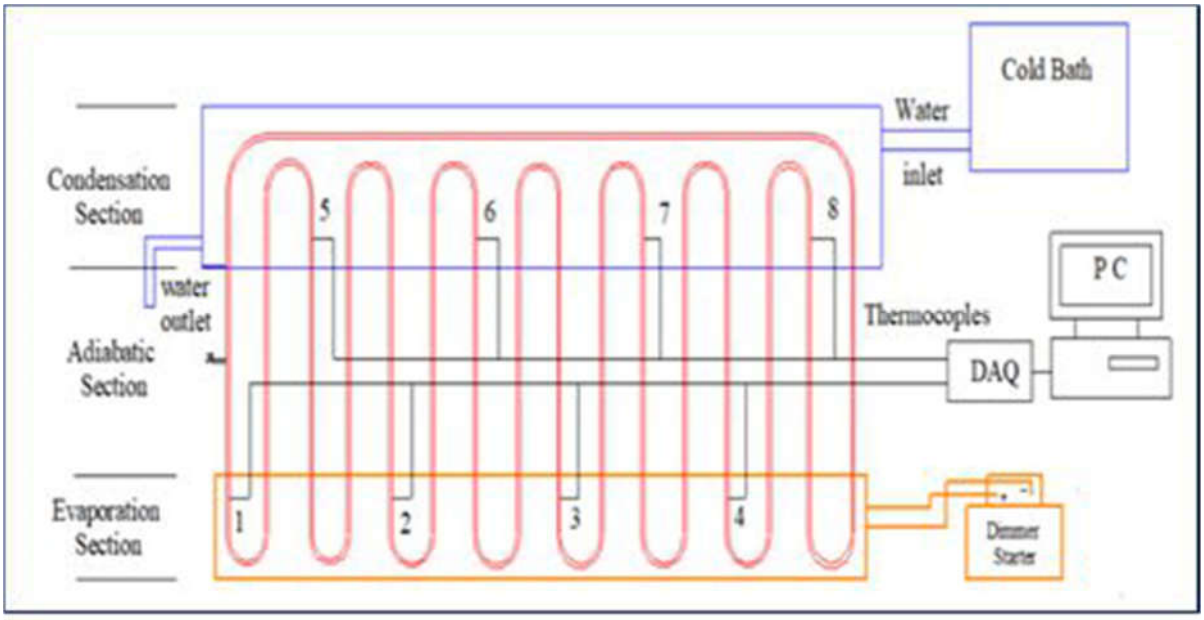

Fig 6. PHP Diagram of the test setup system.

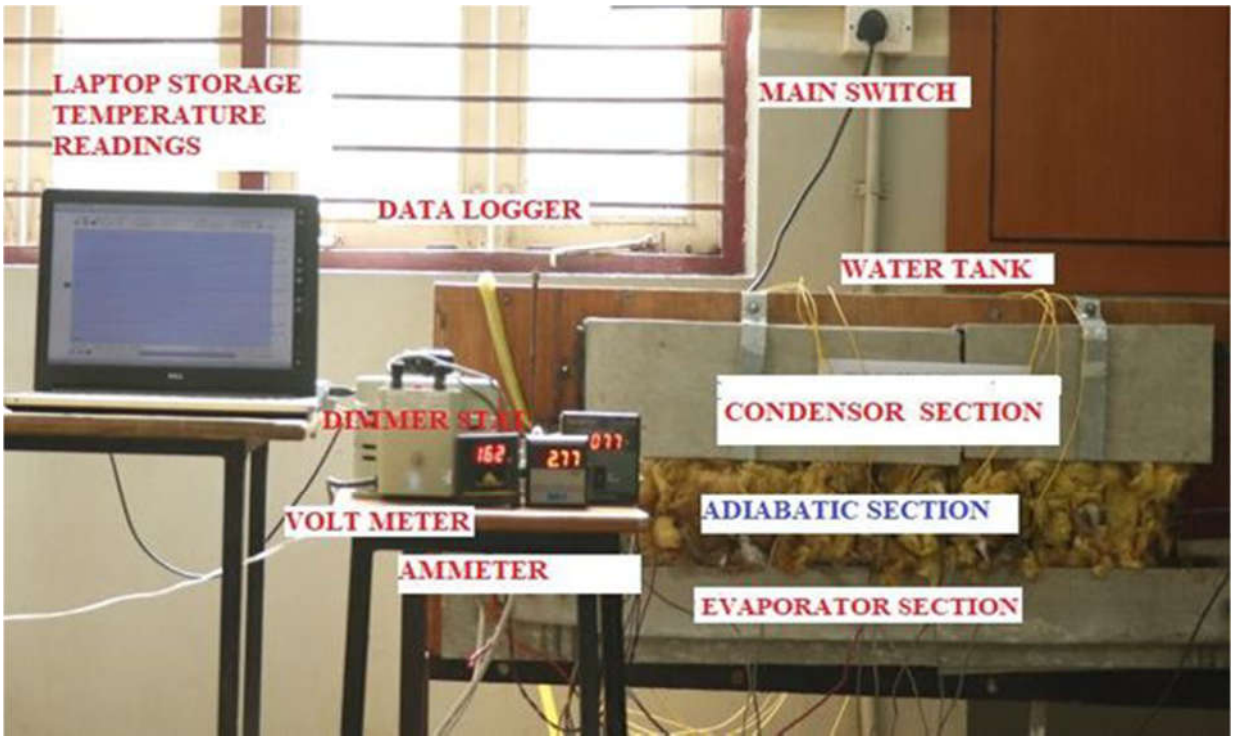

Fig 7. Pulsating Heat Pipe test setup.

Figure 6 and 7 shows schematic block diagram and experimental setup of eight loops PHP. In this experiment copper pipe having inside distance of 3mm and outer thickness 4mm with thickness 1mm were adopted. Copper have been used due to high thermal conductivity. PHP section is dividing into three zones, the main supply of heat input in Evaporator Section, Adiabatic Section where no heat is absorbed or rejected where glass wool is used as a insulator and heat rejected in condenser section. The evaporator section involves of a flat plate heater of size 60x120mm with a maximum capacity 2000W. The power supply to the heater with a varying voltage from 0 to 230V is adopted. The temperature variations inside the pulsating heat pipe dignified using DAQ system connected through laptop. This system connected with different thermocouples like T4, T3, T2, T1 (Evaporator Section), T8, T7, T6 and T5(Condensers Section) respectively. The analog data obtained during experimentation is converting into digital form using DAQ system accompanying with the system as shown in figure 3. The setup consisting of wooden stand with steel support and flat plate heater with enclosing glass wool asbestos and entire system was cooled by supplying continuous water with flow rate of 0.0032 kg/sec. as a working fluid filled inside the pipe with percentage varying from 45%,55%, 65%, 75% and 85% respectively. Heat generation in evaporator section by a dimmer stat varying in flat plate heater is 120W, 240W, 360W, 480W and 600W by a step size of 120W. Experiments were conducted for individual parameters with respect to time, once temperature increases in evaporator section then pulsations inside the PHP was observed and once steady state is reached, continuous pulsations in evaporator region to condenser section was observed.

6.Results and discussion.

6.1.Effect of evaporator section length on PHP performance.

The average thermal resistance of PHPs with regard to the difference between condenser temperature and evaporator temperature may be calculated by equation 7. As may be seen in fig 3, if the condenser section is extended, the ability of PHP to transfer heat will increase since PHP has a greater thermal resistance as gets larger. There are two reasons why these phenomena may exist. Firstly, the length of PHP does not change, but the length ratio does. This results in a smaller length of the evaporation section and more working fluid in adiabatic sections. Due to the pressure difference between the evaporation section and the condensation section, more working fluid with a low temperature needs to be pushed to flow. This increases the resistance of the working fluid circulation in the PHP. The average temperature in the evaporation section increases as the section becomes shorter. This is due to an increase in the heat flow per unit area and a constant heating power. The thermal resistance in the PHP increases even though the temperature in the condensation section remains constant.

6.2.Effect of convective heat transfer coefficient of evaporator section on PHP

performance

6.2.1. Start-up performance.

The CFD models of the PHPs with different length ratios are built based on the section lengths of the PHPs listed in Table 1. They are heated with a heating power of 50 W for the first 800 seconds. With a heating power of 50 W, the calculation shows how the length ratio affects the start-up time in the region of Fig 8. This section shows how the evaporation portions of the average temperature of the PHPs have changed over time Fig 9. As can be observed, the start-up time decreases as the length ratio increases with a fixed heating power. It indicates that extending the adiabatic phase can improve the PHP's start-up performance.

The primary causes of this are two in number. Firstly, with an increase in the length ratio "i.a," the length of the evaporation section reduces, and this, in turn, does not increase the length of the PHP as a whole. The liquid columns in the evaporation section will be able to absorb more heat in a unit of time and convert to more vapour plugs with a reduction in length of this section, as the heating power is constant in this section. As a consequence of this, on one hand, the differential in temperature between the evaporation and condensation regions is likely to increase. However, this is also likely to cause an increase in the volume % of the vapour phase in the evaporation phase. As a consequence of this, the working fluid is likely to travel faster from the evaporation stage to the condensation stage, thereby reducing the start-up time.

Second, with an increase in the length ratio "ia," there is a reduction in length in the condensation section, leading to a reduction in heat dissipation area. There is a reduction in the amount of heat that can be lost in the condensation section due to constant temperature, and this forces the evaporation section to generate energy, which reduces the time of startup.

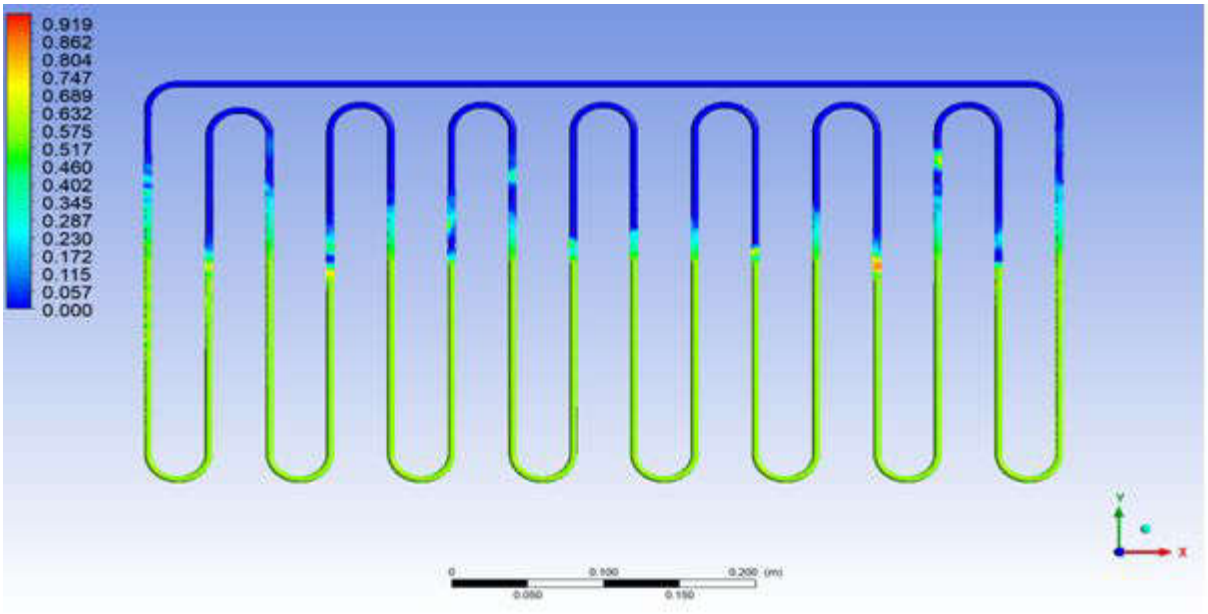

Fig 8: Volume of fraction two turn PHP.

6.2.2. Dry-out: inverse flow dynamics and reduced heat transfer.

Fig.8. As soon as the vapour pressure of the water reaches the operating pressure, it is stated to boil in the PHP. The model of evaporation and condensation is set to attain the saturation temperature at which the water boils at 35°C (308 K). In spite of the fact that the vapour pressure of the water is 5626.20 Pascal at 35°C, various attempts are made to test the numerical model by using various characteristics of boiling in dry-out occurrences, ranging from 2 to 10 kPa. Due to the delayed start-up in the boiling, it is found that the dry-out phenomenon happens at a slower rate at the evacuated pressures below 5636.20 Pascal. In the same way, it is found that the dry-out occurrences of the working fluid are at a faster rate at the operating pressures above 5626.20 Pascal.

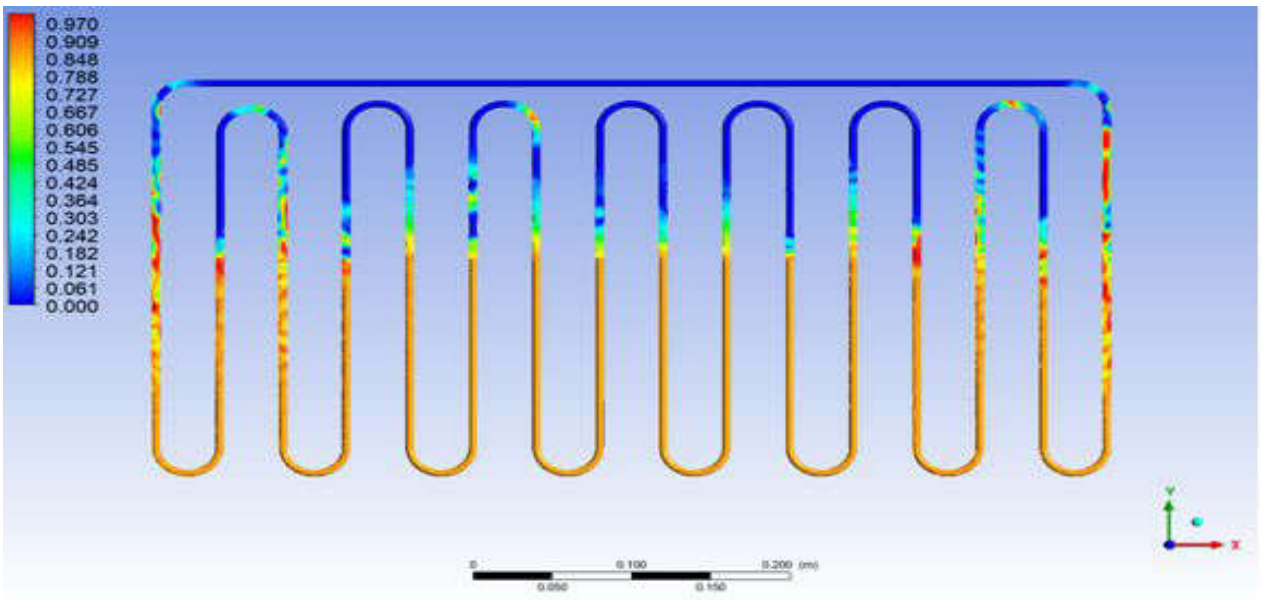

Fig: 9 Heat Input 30w (v/s) Fill Ratio 50 % (phase of mixture)

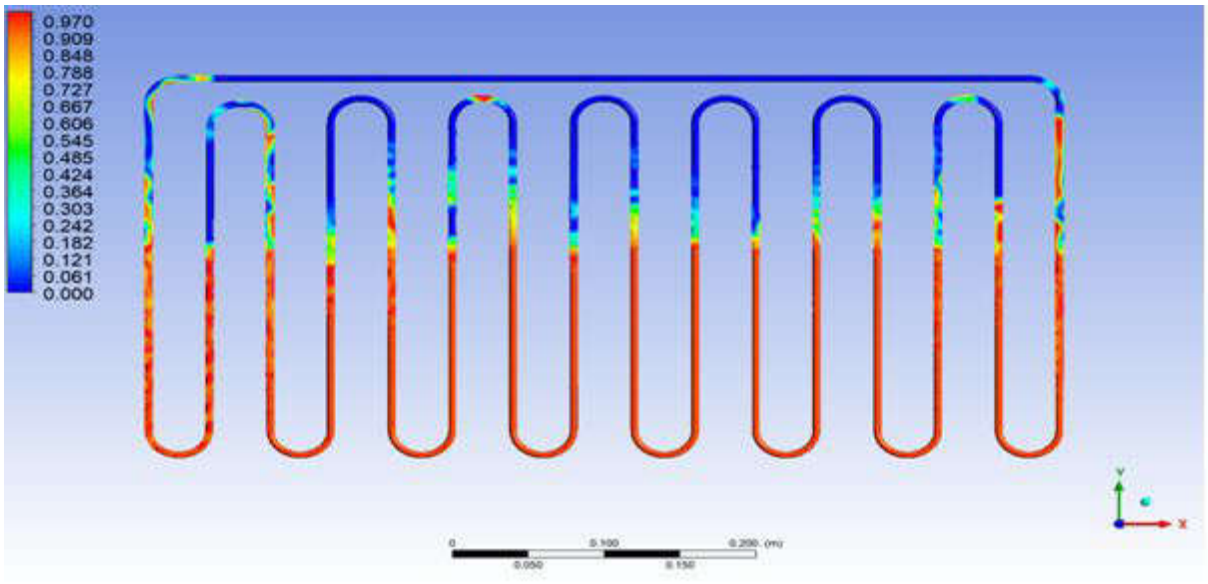

Fig: 10 Heat Input 30w (v/s) Fill Ratio 50 % (phase of vapour)

6.2.3. Evaporator Temperature v/s heat input for Dowtherm A.

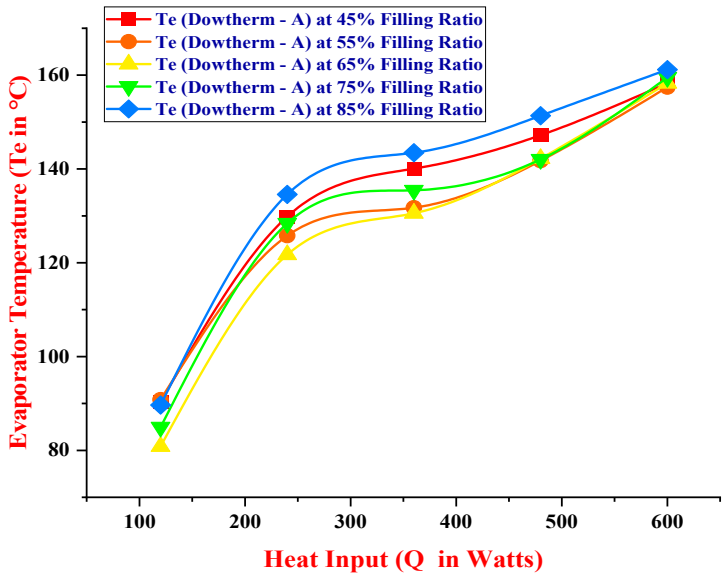

Fig.11. Evaporator Temperature v/s heat input for Dowtherm A.

Figures.11 display the dissimilar temperature of the evaporator resulting from heat input for Dowtherm A with filling ratios of 45%, 55%, 65%, 75% and 85% independently. That the

evaporator temperature is very low at low heat input and increase the heat input for the filling ratios invested. If the temperature of the evaporator grows, the vapor bubbles and the liquid plugs into the pulsating heat Pipe Speed up, which enhances the convective heat flow and, as a result, further increases the heat transferred through the sensible heat. When comparing the evaporator temperature for various intermediate temperature fluid Dowtherm A

6.2.4 Condensor Temperature v/s heat input for Dowtherm A.

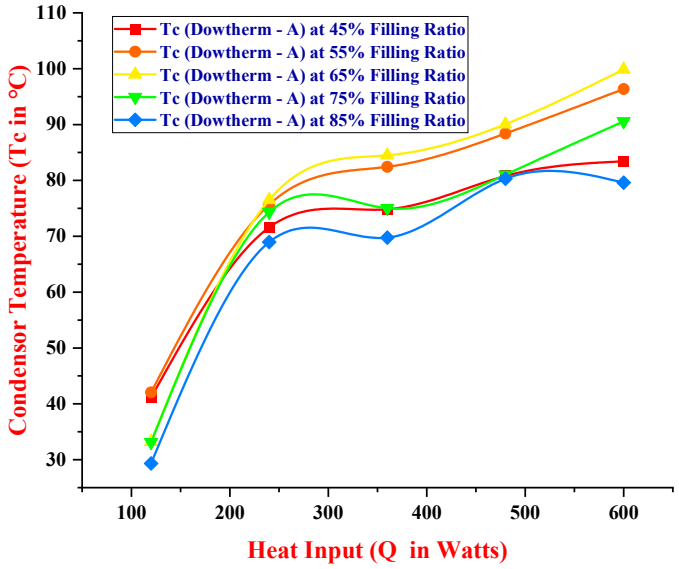

Fig.12. Condenser Temperature v/s heat input for Dowtherm A.

Figure.12 indicates differences in condenser temperatures along with heat input for Dowtherm A filling ratios of 45%, 55%, 65%, 75% and 85% respectively. condenser temperatures are seen to be very low at a lower heat input and an increase in heat input. The condenser temperatures are lower due to the very slow and intermittent motion of the working fluid at the lower heat input. Because of lower energy levels, the flow of the working fluid is reasonable at lower heat inputs. Hot working fluid takes far longer to enter the condenser region from the evaporator portion. The more heat supply, the more fluid oscillations within Pulsating Heat Pipe and thus more heat transfer rate.

6.2.5. Evaporator Temperature v/s heat input for Dowtherm A.

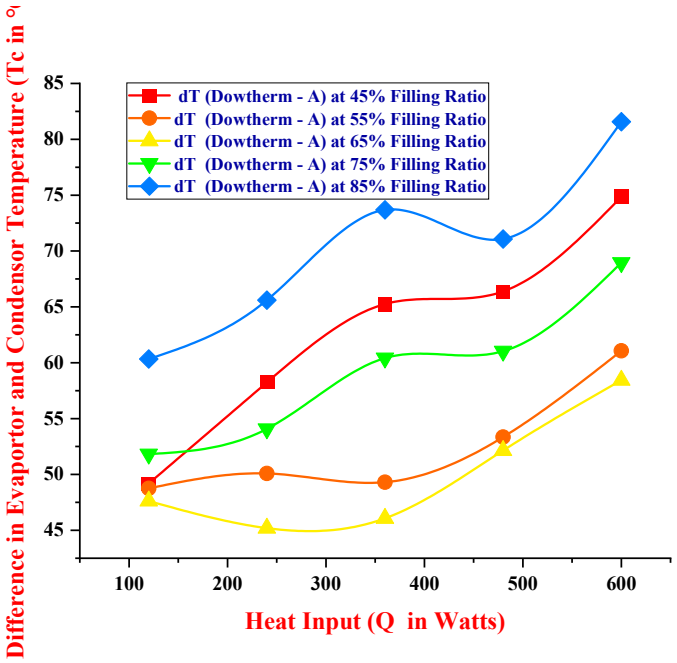

Fig.13. Temperature difference between Evaporator and condenser heat input for Dowtherm A.

Figures.13 display differences in temperature differential between evaporator and condenser at various heat inputs for Dowtherm –A with a filling ratio of 45%, 55%, 65%, 75% and 85% respectively. Figures 8 an demonstrate that the temperature variations between the evaporator and the condenser are considerably smaller at the lower heat input as the fluid flow is mild at the lower heat input, which is combined with a lot of variability. The temperature differential between the evaporator and the condenser is higher absorption of heat. Vapor bubble formations control the pumping activity in the pulsating heat pipe. If the bubbles are higher in PHP, the heat transfer rate is also higher in the evaporator portion and the condenser section.

6.2.6. Thermal Resistance v/s Heat Input in Q Watts

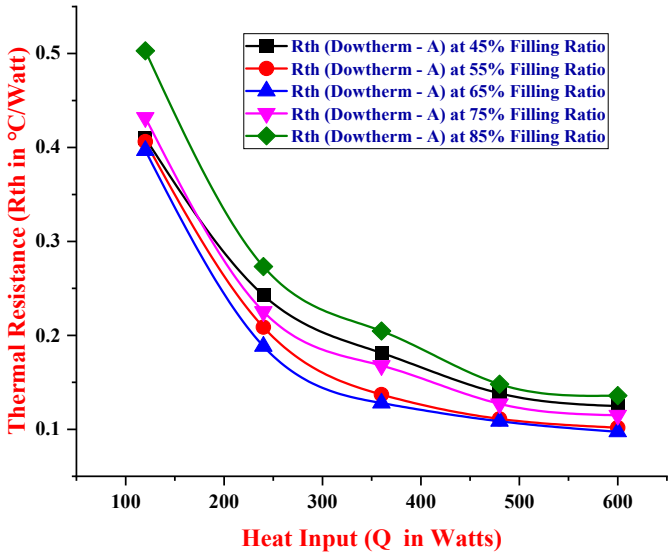

Fig.14.Evaporator Temperature v/s heat input for Dowtherm A.

Figures.14 show the effective thermal thermal resistance v/s heat input for working fluids Intermediated temperature fluids Dowtherm A with a filling ratio of 45%, 55%, 65%, 75% and 85% respectively. It is pragmatic that thermal resistance decreases very high during initial heat input due to low pulsation and gradually thermal resistance values. Pulsations commence in the intermediate range of temperatures from 150^0C to 250^0C .

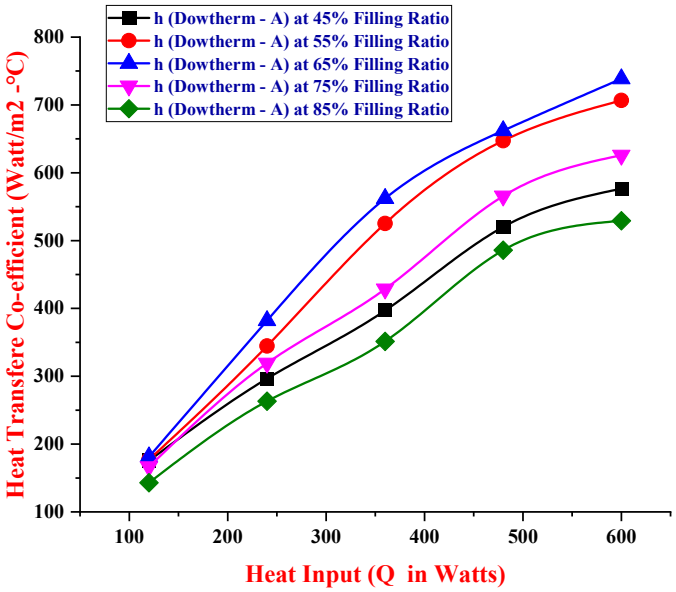

Fig.15. Heat transfer Co-efficient v/s heat input for Dowtherm A.

Figures.15 demonstrate the effect of heat intake on the heat transfer co-efficient of PHP for various intermediate temperature working fluids such as Dowtherm A with a filling ratio of 45%, 55%, 65%, 75% and 85% respectively. The co-efficient heat transfer of PHP is observed to increase with an increase in heat input. The heat in the evaporator portion rises moderately with time and the fluid is transformed from a liquid to a vapor state by reducing its mass. The heat supply of the thermo-fluidic motion engine. As a result, increasing pumping power improves the efficiency, and further, it can be shown that Dowtherm A with a 65% filling ratio show higher heat transfer coefficients compared to filling ratios.

6: Conclusion.

The numerical method employed in the current investigation is entirely based on liquid-vapor dynamics and the correct concept of the operational limits applicable to closed-loop PHPs employing water as the working fluid (standardized data).

1. The authors are trying to apply the cutting-edge concepts (inverse flow dynamics) to other practical fluids. These new concepts may be more applicable to dry-out limits in PHPs when they are validated with various operating fluids. As several experts have pointed out, the fill ratio of 50% cannot be harmonized for various working fluids. Fill ratio is seen to be a robust function of the physical and thermal parameters of the working fluid and the PHP's size.
2. Dry-out: From the above figure, it is clear that abnormal velocity of fluids is a common phenomenon in all three parts of the PHP due to a buildup of initial pressure in the evaporator section and impulsive pressure release after startup.
3. This phenomenon is the main reason for the dry-out of the PHP.
4. The dry-out limit of PHPs is increased due to the temporal rate of change of the volume fraction of the liquid and the vapor in each of the three parts of the PHP, as per the equivalence point research.
5. The more time it takes to dry out, the less quick the drying process is. The volume fraction of the vapor increases, and the volume fraction of the liquid water decreases. Therefore, several criteria that can be examined to determine the dry-out phenomenon in PHPs include changes in pressure and volume fraction of the vapor and liquid water in the different parts of the PHP.
6. Increase the heat input and decrease the Thermal Resistance in Dowtherm – A Intermediate Temperature Fluids.

7. In Dowtherm-A Intermediate Temperature Fluids, raise the heat input and lower the thermal resistance.

7.Reference

1. Wang, X., Shi, Y., Liu, T., Wang, S., Wang, K., Chen, H., ... & Zhu, Y. (2022). CFD modeling of liquid-metal heat pipe and hydrogen inactivation simulation. *International Journal of Heat and Mass Transfer*, *199*, 123490. https://doi.org/10.1016/j.ijheatmasstransfer.2022.123490.
2. Zhang, D., He, Z., Guan, J., Tang, S., & Shen, C. (2022). Heat transfer and flow visualization of pulsating heat pipe with silica nanofluid: An experimental study. *International Journal of Heat and Mass Transfer*, *183*, 122100.

https://doi.org/10.1016/j.ijheatmasstransfer.2021.122100.

3. Li, S., Sun, X., Liu, D., Jiao, B., Pfotenhauer, J., Gan, Z., & Qiu, M. (2022). Experimental study on a hydrogen pulsatingheat pipe in different heating modes. *Cryogenics*, *123*, 103440. https://doi.org/10.1016/j.cryogenics.2022.103440.
4. Barba, M., Bruce, R., Bouchet, F., Bonelli, A., & Baudouy, B. (2021). Effects of filling ratio of a long cryogenic Pulsating Heat Pipe. *Applied Thermal Engineering*, *194*, 117072. https://doi.org/10.1016/j.applthermaleng.2021.117072.
5. Fonseca, L. D., Miller, F., & Pfotenhauer, J. (2015, November). Design and operation of a cryogenic nitrogen pulsating heat pipe. In *IOP Conference Series: Materials Science and Engineering* (Vol. 101, No. 1, p. 012064). IOP Publishing. doi:10.1088/1757-899X/101/1/012064.
6. Kang, Z., Shou, D., & Fan, J. (2022). Numerical study of single-loop pulsating heat pipe with porous wicking layer. *International Journal of Thermal Sciences*, *179*, 107614. https://doi.org/10.1016/j.ijthermalsci.2022.107614.
7. Pachghare, P. R., & Mahalle, A. M. (2014). Thermo-hydrodynamics of closed loop pulsating heat pipe: an experimental study. *Journal of Mechanical Science and Technology*, *28*(8), 3387-3394. https://doi.org/10.1007/s12206-014-0751-9.
8. Błasiak, P., Opalski, M., Parmar, P., Czajkowski, C., & Pietrowicz, S. (2021). The Thermal—Flow Processes and Flow Pattern in a Pulsating Heat Pipe-Numerical Modelling and Experimental Validation. Energies, 14(18), 5952 https://doi.org/10.3390/en14185952
9. Bae, J., Lee, S. Y., & Kim, S. J. (2017). Numerical investigation of effect of film dynamics on fluid motion and thermal performance in pulsating heat pipes. Energy Conversion and Management, 151, 296-310. https://doi.org/10.1016/j.enconman.2017.08.086
10. Celata, G. P., Cumo, M., Dossevi, D., Jilisen, R. T. M., Saha, S. K., & Zummo, G. (2012). Flow pattern analysis of flow boiling inside a 0.48 mm microtube. *International journal of thermal sciences*, *58*, 1-8. https://doi.org/10.1016/j.ijthermalsci.2012.03.014

11. Spinato, G., Borhani, N., & Thome, J. R. (2015). Understanding the self-sustained oscillating two-phase flow motion in a closed loop pulsating heat pipe. *Energy*, *90*, 889-899. https://doi.org/10.1016/j.energy.2015.07.119
12. Zhang, Y., & Faghri, A. (2008). Advances and unsolved issues in pulsating heat pipes. *Heat Transfer Engineering*, *29*(1), 20-44. http://dx.doi.org/10.1080/01457630701677114
13. Rudresha, S., & Kumar, V. (2014). CFD analysis and experimental investigation on thermal performance of closed loop pulsating heat pipe using different nanofluids. *International Journal of Advanced Research*, *2*(8), 753-760.
14. Holley, B., & Faghri, A. (2005). Analysis of pulsating heat pipe with capillary wick and varying channel diameter. *International journal of heat and mass transfer*, *48*(13), 2635-2651. https://doi.org/10.1016/j.ijheatmasstransfer.2005.01.013
15. Cui, X., Zhu, Y., Li, Z., & Shun, S. (2014). Combination study of operation characteristics and heat transfer mechanism for pulsating heat pipe. *Applied Thermal* https://doi.org/10.1016/j.applthermaleng.2014.01.030
16. Kang, Z., Shou, D., & Fan, J. (2021). Numerical study of a novel Single-loop pulsating heat pipe with separating walls within the flow channel. *Applied Thermal Engineering*, *196*, 117246. https://doi.org/10.1016/j.applthermaleng.2021.117246.
17. Rudresha, S., & Babu, E. R. (2019). Experimental Investigation on the Thermal Performance of a Pulsating Heat Pipe by using TiO2 with Dowtherm A Nanofluids. In Proceedings of the 25th National and 3rd International ISHMT-ASTFE Heat and Mass Transfer Conference (IHMTC-2019). Begel House Inc. **DOI:** 10.1615/IHMTC-2019.470.
18. Rathinam, R., Singh, D. P., Dutta, A., Rudresha, S., Ali, S. R., & Chatterjee, P. (2022). TiO2 Nanoparticles Based Peroxidase Mimics for Colorimetric Sensing of Cholesterol and Hydrogen Peroxide. In *Advances in Science and Technology* (Vol. 117, pp. 85-90). Trans Tech Publications Ltd. **https://doi.org/10.4028/p-7in58j**

****